

## PHYSICAL AND NUMERICAL INVESTIGATIONS OF MOULD FLUX ENTRAINMENT INTO LIQUID STEEL

This paper presents results of model tests, performed in order to analyze phenomenon of slag droplets entrainment into steel in mould, during continuous casting process. The carried out studies took the form of laboratory experiments using physical model, in which – using similarity criteria – the behaviour of interfacial boundary liquid steel-liquid slag has been simulated using water and silicon oils, differing in physicochemical properties. Additionally, based on PIV (Particle Image Velocimetry) measurements and numerical simulations, vector flow field and values of critical velocities, at which observed the occurrence of interfacial boundary silicon oil-water instability have been identified. Based on the carried out investigations, results, that illustrate relationship between critical entrainment velocity and physicochemical properties of oils have been presented.

*Keywords:* slag entrainment, Kelvin-Helmholtz instability, water-oil investigations, numerical simulation, particle image velocimetry.

### 1. Introduction

Continuous casting is the leading method of semi-finished steel production. Machine used to this process consists of: ladle, tundish, mould and secondary cooling zone, with system of bending and straightening rollers. Mould is one of the key elements of continuous casting machine, whose correct operation has a significant impact on the final quality of cast billet, bloom or slab. During the casting process, the mould powder is given on the surface of liquid steel, located in the mould working volume. As a result of contact with hot, liquid metal, layer of mould powder melts and forms a slag layer, which fulfills series of tasks, affecting the proper operation of mould and having a major impact on the semi-finished steel product quality: prevents welding of continuous ingot to mould's walls due to providing of lubrication, assimilates some of the nonmetallic inclusions, protects the liquid steel from oxidation as a result of contact with air atmosphere, controls the intensity of heat dissipation [1, 2, 3]. Hydrodynamic conditions in the mould have a significant impact, whether slag properly fulfills its role. The behaviour of interfacial boundary liquid steel-liquid slag is a dynamic process, dependent on such factors as: casting speed, shape and dimensions of mould, geometry of submerged entry nozzle, submergence depth, amplitude and frequency of oscillatory motion of the mould, physicochemical properties of liquid steel and liquid slag, interfacial tension between this two phases. Improper selection of continuous steel casting process variables can lead to instabilities of boundary layer and liquid slag portions entrainment into liquid steel volume. Drops of entrained slag can: flow back into the slag layer, circulate in a liquid steel volume or accumulate on the front

of crystallization, polluting and lessening the quality of the cast continuous semi-finished product. For this reason, the behaviour of liquid slag layer on the liquid steel surface in mould is an important and often investigated problem of modern continuous steel casting process. The research take different forms, including plant measurements [4, 5], investigations – basing on the similarity numbers: Weber (We), Froude (Fr), Reynolds (Re) and Capillary (Ca) – using the oil-water physical models [6, 7] and also numerical simulations [8, 9].

Based on the results of research over the years, the following mechanisms of liquid slag droplets entrainment were proposed [10]:

1. shear-layer Kelvin-Helmholtz instabilities (KHI),
2. fluctuations of top surface,
3. Karman vortex formation near submerged entry nozzle,
4. meniscus freezing and hook formation,
5. flow of Ar bubbles,
6. stationary wave instability, forming on the top surface,
7. exposing the liquid steel surface near the narrower wall of mould.

### 2. Shear layer instability, mathematical models

Slag passing into the liquid steel in the mould due to the instability of the interfacial boundary is caused mainly by the occurrence of the so-called Kelvin-Helmholtz phenomenon, which is also observed in nature, e.g. during the formation of sea waves. The KHI phenomenon occurs, when there is a difference in velocity between two contacting phases, differing also in specific density.

\* CZĘSTOCHOWA UNIVERSITY OF TECHNOLOGY, FACULTY OF PRODUCTION ENGINEERING AND MATERIALS TECHNOLOGY, DEPARTMENT OF METALS EXTRACTION AND RECIRCULATION, 19 ARMII KRAJOWEJ AVE., 42-200 CZĘSTOCHOWA, POLAND

<sup>#</sup> Corresponding author: jowsa@wip.pcz.pl

The entrainment of slags due to the occurrence of the KHI mechanism has been the subject of numerous studies [6, 10, 11], which provide laboratory tests results and relationships defining the critical velocities of the entrainment of the lighter phase (oil or slag) to the heavier phase (water or steel). The most critical review of those relationships has been done in this study [10]. The KHI phenomenon is described by both theoretical and empirical relationships (models). The theoretical relationships have simple solutions solely for inviscid liquids; in the case of viscid liquids, solutions are very complex, therefore relationships in the form of less complex empirical models are often given. Among theoretical relationships, the classic equation [12]:

$$(V_{1cr} - V_{2cr})^2 \geq \frac{2(\rho_1 + \rho_2)}{\rho_1 \rho_2} \left( \sqrt{(\rho_2 - \rho_1) g \sigma_{12}} \right) \quad (1)$$

and the equation given by Milne-Thompson [13]:

$$(V_{1cr} - V_{2cr})^2 = (\rho_2 - \rho_1) g (H_1 / \rho_1 + H_2 / \rho_2) \quad (2)$$

where:  $\rho$  – density [kg/m<sup>3</sup>],  $\sigma_{12}$  – interfacial tension [N/m],  $g$  – acceleration due to gravity [m/s<sup>2</sup>],  $H$  – depth of liquid layer [m],  $V_{cr}$  – critical velocity [m/s], index <sub>1</sub> - upper liquid, index <sub>2</sub> - lower liquid,

should be mentioned.

On the other hand, from among many empirical relationships, that have been derived based on various measuring techniques, relationship 7 according to the publication [10] should be quoted, because it is considered as best describing the experimental data reported therein:

$$V_{cr} = c \frac{\sigma_{12}^{0.292} g^{0.115} (\rho_2 - \rho_1)^{0.215} \mu_1^{0.231}}{H_1^{0.365} \rho_1^{0.694} \mu_2^{0.043}} \quad (3)$$

where:  $\mu$  – dynamic shear viscosity [Pa·s],  $c=3.065$  is dimensionless constant.

Two empirical relationships should also be referred to, which have been obtained in recent years by the team of Professor Scheller [6, 7] upon using the „single-roller driven flow” technique:

$$V_{cr} = c_1 \frac{\sigma_{12}}{\mu_2} \exp\left(c_2 \frac{v_1}{v_2}\right) \quad (4)$$

where  $v = \mu/\rho$  kinematic shear viscosity [m<sup>2</sup>/s],  $c_1 = 0.0233$  and  $c_2 = 0.001$  are dimensionless constants.

$$V_{cr} = \frac{\sigma_{12}}{\mu_2} \left( c_1 + c_2 \frac{v_1}{v_2} \right) \quad (5)$$

where  $c_1 = 2.8 \cdot 10^{-3}$  and  $c_2 = 3 \cdot 10^{-6}$  are dimensionless constants.

Using these formulae, the values of the critical velocity were calculated for the conditions of the author’s planned experiment, and are given in Table 1.

The most important physicochemical properties of oils used in experiments are shown in Table 2.

It can be noticed from the results presented in the Table 1, that there occur significant differences in critical velocities, especially for equations 3 and 4 they are much higher than for the other cases. For this reason, a decision was made to undertake the author’s own studies to determine the critical velocity, when the entrainment of the lighter phase (oil) to the heavier phase (water) occurs.

Predictions of critical velocities ( m/s) for oil – water system

TABLE 1

Oil type	$V_{cr}$ [m/s]				
	Eq. no. 1	Eq. no. 2	Eq. no. 3	Eq. no. 4	Eq. no. 5
<b>Polsil OM20</b>	0.136	0.195	0.658	1.059	0.127
<b>Polsil OM50</b>	0.127	0.168	0.618	1.122	0.135
<b>Polsil OM100</b>	0.124	0.159	0.607	1.214	0.146
<b>Polsil OM300</b>	0.123	0.154	0.607	1.587	0.185
<b>Polsil OM500</b>	0.121	0.149	0.598	1.979	0.218
<b>Polsil OM1000</b>	0.117	0.139	0.579	3.437	0.299

The most important physicochemical properties of silicon oils used in experiments (in temperature 25°C)

TABLE 2

Oil type	Density [g/cm <sup>3</sup> ]	Kinematic viscosity [cSt]	Dynamic viscosity [Pa·s]
<b>Polsil OM20</b>	0.947	20	0.01894
<b>Polsil OM50</b>	0.960	50	0.048
<b>Polsil OM100</b>	0.964	100	0.096
<b>Polsil OM300</b>	0.966	300	0.2898
<b>Polsil OM500</b>	0.968	500	0.484
<b>Polsil OM1000</b>	0.972	1000	0.972

### 3. Research methodology

Investigations, in order to determine critical velocity of heavier phase (water or steel), which cause the occurrence of lighter phase (oil or slag) droplets entrainment due to KHI, were divided into three parts. First of them takes the form of tests, based on a physical model of top part of mould, where liquid steel has been replaced by water, while liquid slag layer – covering her surface – has been replaced by silicon oils.

The conditions of conducting the model studies of slag entrainment to the steel should satisfy simultaneously two criteria expressed with the Froude number and the Weber number. The condition of satisfying the Froude number is commonly used in modelling of steel casting in the mould. On the other hand, the Weber number, in the form of the expression:

$$We = \frac{V^2 L \rho_2}{\sigma_{12}} \quad (6)$$

where :  $L$  - characteristic length [m],

is used for a multi-phase flow, where one fluid borders the other, and where the interface surface may be curved, e.g. through the entrainment of drops of one fluid to the other. When the Froude and Weber number are considered, the scale factor for the case under consideration is:

$$\lambda = \frac{L_{water-oil}}{L_{steel-slag}} = \sqrt{\frac{\rho_{steel} \sigma_{water-oil}}{\rho_{water} \sigma_{steel-slag}}} \approx 0.5 \quad (7)$$

On this basis, the thickness of silicon oil covering the water in the test vessel will be determined.

According to the similarity theory, water at temperature of 25°C has the similar value of kinematic viscosity to that of liquid steel, so under turbulent motion conditions both liquids behave similarly. Physical model used in tests, made of plexiglas, has a cuboid shape. Inside the model located baffles, whose task is directing stream of water tangentially to the oil layer. Scheme of the discussed model is presented in Fig. 1.

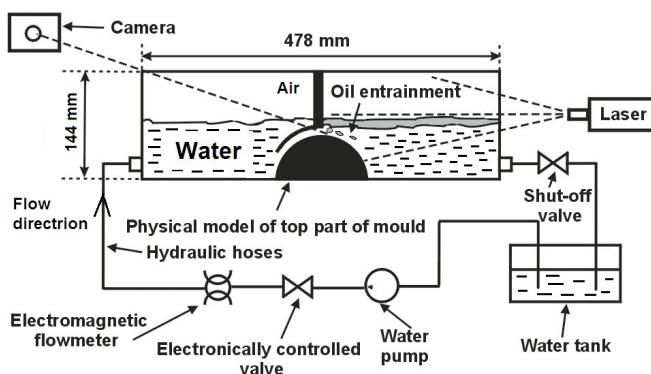


Fig. 1. Scheme of physical model used in laboratory experiments

The continuity of water flow, necessary to carry out tests, was guaranteed by applying control system, consisting of pump, flow control valves, electromagnetic flowmeter, hydraulic connections system and tank, acting as reservoir of water. Experiments were performed in this manner, that - after stabilization low-intensity water flow (3.0 l/min) - on the

surface of heavier phase, oil layer with the thickness of 8 mm was placed. In the next step, gradually increased water flow-rate, caring – after each increase – to stabilize water flow and to maintain the constant distance between oil layer and bottom wall of model. Water flow rate increased, until the instability of boundary layer water-silicon oil and the phenomenon of oil droplets entrainment were observed. The critical values of water flow rate were noted. The course of experiments recorded using high-speed camera and photo camera.

The second step of studies aimed at numerical modeling of interfacial boundary instabilities phenomenon and determining critical values of velocities. Simulations were performed using commercial code Ansys-Fluent®. Before proceeding to the essential calculations, it was necessary to create virtual replica of physical model of top part of mould. For this purpose, program Gambit was used. Because the object under investigations have a symmetry plane, it was decided, that only one half of them will be applied in calculations, which will allow to decrease their time. Next, virtual model was exported to application Ansys-Meshing®, in which structural discretization grid, consisting of 749 thousand elements, was created. In order to increase accuracy of calculations, computational mesh was concentrated near the walls of the object. In the further step of research, virtual object with computational mesh was exported to CFD (Computational Fluid Dynamics) program. The following boundary conditions were assigned to the virtual model: **mass flow inlet** – for the cross-section of spigot, through which water is supplied, **outflow** – cross-section of spigot, through which water is drain, **symmetry** – for the symmetry plane of the object, **slip wall** (wall with zero stress) – for model's top wall, **wall** – for all other walls. It was assumed, that 6 calculations will be carried out for one-phase system and one for three-phase system, including water, oil Polsil OM20 and air. Simulations using one-phase system conducted in this manner, that for each of them set water flow rate equal critical water flow rate, obtained by physical experiments. For three-phase simulation set water flow rate equal 8.0 l/min (flow rate at which interfacial boundary instabilities occurred). Turbulent motion of fluids described using the Realizable  $k-\epsilon$  turbulence model. For coupling pressure and velocity fields, the Semi-Implicit Method for Pressure-Linked Equations-Consistent (SIMPLEC) algorithm was chosen. The pressure field was solved using the PRESTO! method. In order to modeling the behaviour of silicon oil-water interfacial boundary, the most popular model to front tracking – VOF – was selected. For water and air phases, the physicochemical properties were taken from Ansys-Fluent® database - water density: 998.2 kg/m<sup>3</sup>, water viscosity: 0.001 Pa·s, air density: 1.225 kg/m<sup>3</sup>, air viscosity: 1.789·10<sup>-5</sup> Pa·s, while oil properties set in accordance with table no. 2. The value of oil-water interfacial tension set as equal 0.04 N/m, according to data in publication [6]. For spatial variable discretization, the Modified HRIC interface tracking scheme will be proper, while for temporal variable discretization, Implicit scheme may be used. These schemes provides clear mapping of interfacial boundary, while maintaining relatively short time of computation. Computation were performed for isothermal conditions, in a transient state, with a time step of 0.01s. The solution of continuous-differential equations was considered convergent, when the values of all residues fell below the value 10<sup>-3</sup>.

The third stage of this study was to determine vector velocity field, on the basis of physical model measurements. For this purpose, the 2DPIV (2D Particle Image Velocimetry) vector flow field recording and analysis system, located in Department of Metal Extraction and Recirculation at Czestochowa University of Technology, was used. The detailed description of the system can be found in paper [14]. The idea of this measurement method is the introduction of glass balls into water flowing through the physical model and lighting them by laser beam. Then, using the 2DPIV module, the recorded by camera ball motion is transformed into the vector velocity field. During a single measurement, 46 images (in double photo-frame mode, i.e. for each image falls two photo-frames) were recorded with frequency equal 15 images per second and time interval between two frames equal 100 microseconds.

#### 4. Results

Based on the laboratory tests, carried out on a physical model (Fig. 1), considering the interaction of the two phases – the silicon oil covering the water surface and the water flowing through the vessel at a variable flow rate – the effect of the physicochemical properties of the oil and the water flow rate on the behaviour of the oil-water interface was examined. In the conditions of conducting the experiments, two typical situations in interfacial boundary behaviour were observed. The first one, when a stable interfacial boundary exist, with no visible entrainment of oil to the water, and the second one, when an unstable interfacial boundary occurs, with a visible entrainment of oil portions to the water. Transition from one

state to the other occurs, when the critical flow rate of water in the vessel is exceeded. The increase in water flow rate causes an increase in water velocity in the layers immediately adjacent to the oil. The mechanism of oil particles entrainment to the water is explained by the occurrence of the KHI. To illustrate these two states, photographs are shown in Fig. 2. The first of the variants of interfacial boundary formation is illustrated in Fig. 2a, while the other, in Fig. 2b.

It was also observed, that with the change of the silicon oil, the critical water flow rates changed. The higher the oil viscosity, the higher the water flow rate had to be used for the phenomenon of interfacial boundary instability to have occurred. As exceeding a certain critical value of tangential velocity in the region of contact between two phases is one of the driving forces causing the KHI phenomenon, therefore, for each variant of the experiment, its values were estimated using the results of PIV measurements and numerical simulations. The obtained results are given in the Table 3.

For oils of the highest viscosities (Polsil OM500 and Polsil OM1000), it was not possible to determine the velocity field by the PIV method, because, at the critical water flow rate, emulsion formed, which obscured the observation field. Based on the analysis of the vector velocity fields of water, regardless of whether they were obtained by the PIV method or from numerical simulations, the water velocity range was determined in the zone adjacent to the lighter phase in the location of oil drops detachment initiation, that is immediately behind the cylindrically curved channel – tangentially adjoining the oil layer. As an example, velocity fields obtained by the PIV method for the water flow rate of 8 l/min in vessel are shown in Fig. 3 and Fig. 4.

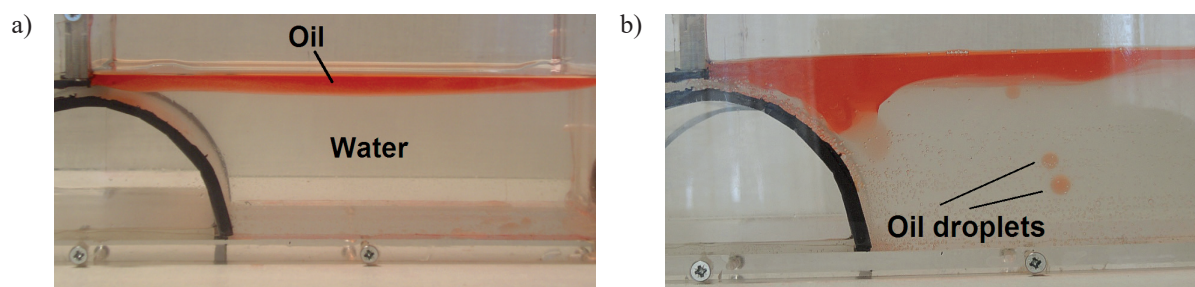


Fig. 2. Two types of interfacial boundary oil – water behaviour: a) stable interfacial boundary, b) unstable interfacial boundary

TABLE 3

Values of critical velocity obtained by numerical simulations and PIV measurements, values of capillary number

Oil type	Critical water flow rate [l/min]	Critical velocity – numerical simulation [m/s]	Critical velocity – PIV measurements [m/s]	Ca <sub>1</sub>	Ca <sub>2</sub>
Polsil OM20	8.0	0.19÷0.22	0.18÷0.22	0.0043	0.0050
Polsil OM50	9.3	0.23÷0.27	0.18÷0.26	0.0050	0.0059
Polsil OM100	10.5	0.26÷0.30	0.22÷0.30	0.0056	0.0064
Polsil OM300	14.4	0.36÷0.42	0.26÷0.38	0.0074	0.0086
Polsil OM500	16.9	0.43÷0.49	-	0.0088	0.0100
Polsil OM1000	19.3	0.48÷0.56	-	0.0098	0.0115



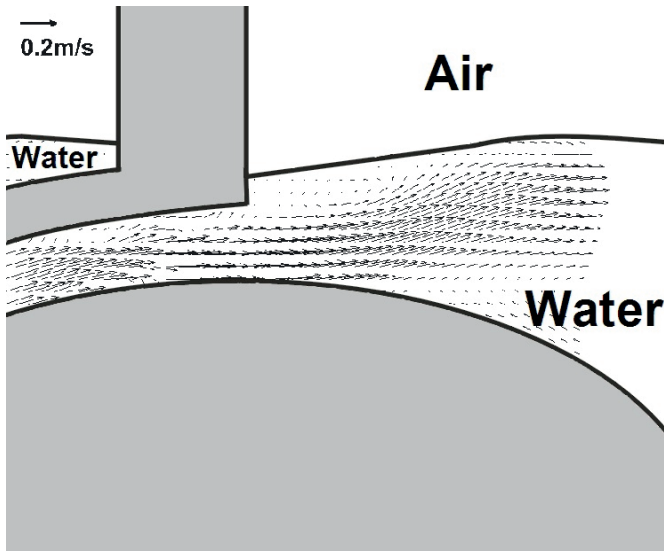


Fig. 3. Vector velocity field obtained by PIV measurements for water flow rate equal 8.0 l/min, case without oil layer

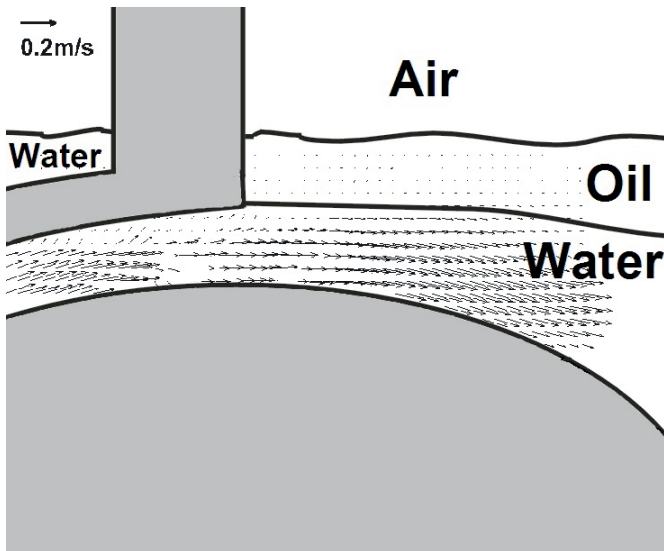


Fig. 4. Vector velocity field obtained by PIV measurements for water flow rate equal 8.0 l/min, case with 8 mm Polsil OM20 oil layer

The numerical simulations results, representing water velocity fields in the vessel under examination, also indicate the locations, in which the water velocity should be red out in the oil drops detachment zone. Fig. 5 shows the situation of single-phase flow in the symmetry plane of the facility under examination, while Fig. 6 illustrates the flow in the multi-phase system in the plane passing in parallel to the plane of symmetry, but shifted by 0.05 m relative to it.

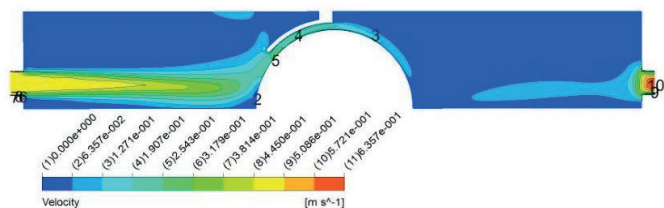


Fig. 5. Velocity field (symmetry plane), case without oil layer, water flow rate equal 8.0 l/min and steady state conditions

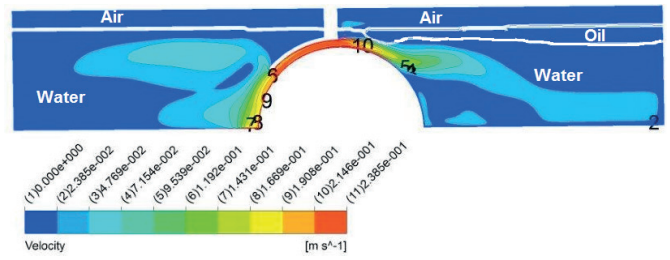


Fig. 6. Velocity field and phases distribution (plane parallel to the symmetry plane, away from it the distance 0.05 m) after 100 sec from start numerical simulation, case with 8 mm Polsil OM20 oil layer and water flow rate equal 8.0 l/min

The obtained critical water velocities – in the range from the upper limit (1) to the lower limit (2) – enabled the values of the  $Ca_1$  and  $Ca_2$  numbers to be calculated from the following formula:

$$Ca = \frac{V_2 \mu_2}{\sigma_{12}} \quad (8)$$

The values of the  $Ca$  numbers for the performed experiments are given in Table 3.

Using the relationship:

$$Ca \cdot Re = We \quad (9)$$

the values of the Reynolds numbers were calculated in the zone of the occurrence of silicon oil-water interfacial boundary instability. The results, along with the values of the Weber numbers, are given in Table 4. To evaluate the distribution of turbulence in the examined facility, the turbulence intensity was represented in the facility's symmetry plane during the flow of water at a flow rate of 8.0 l/min (Fig. 7). On this basis it can be stated, that the two-phase flow, when the KHI phenomenon comes into play, occurs in the turbulent motion zone.

TABLE 4.

Values of Weber and Reynolds numbers

Oil type	$We_1$	$Re_1$	$We_2$	$Re_2$
Polsil OM20	1.2	1686	9.66	1952
Polsil OM50	10.3	2041	14.2	2396
Polsil OM100	12.85	2307	17.11	2662
Polsil OM300	23.52	3194	32.02	3727
Polsil OM500	33.56	3815	43.58	4348
Polsil OM1000	41.82	4259	56.92	4969

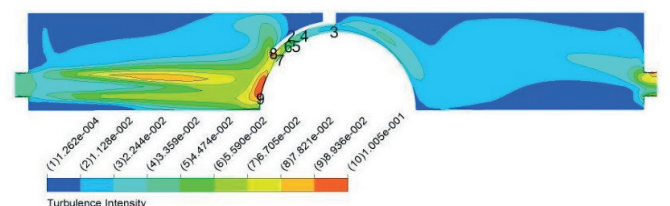


Fig.7. Turbulence intensity field (symmetry plane), case without oil layer, water flow rate equal 8.0 l/min and steady state conditions

Fig. 8 illustrates, based on numerical simulation, the situation in the examined facility at the time of silicon oil drop detachment, which occurred in 36 seconds after the flow rate had been increased to the value of 8 l/min.

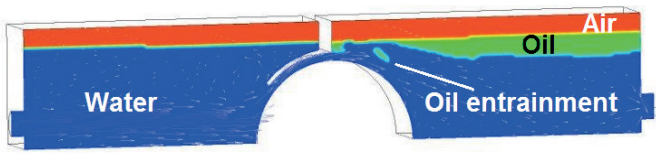


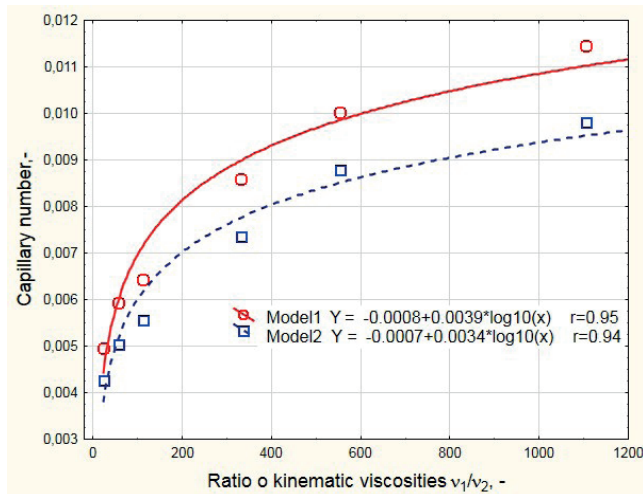
Fig. 8. Oil entrainment phenomenon, observed after 36 sec from increased water flow rate, case with 8mm Polsil OM20 oil layer

a) To find a mathematical model to describe the critical water velocity  $V_{cr}$  as dependent on the experiment conditions, the examination results are shown in Fig. 9 in the form of the Ca number, where the independent variable is the ratio of kinematic viscosities  $\nu_1/\nu_2$ . The results in the chosen coordinate system are very well approximated by nonlinear models with the correlation coefficient  $r \approx 0.95$ . Based on the determined relationships, the models describing the critical velocity for the examined cases are as follows:

$$V_{cr(1)} = \frac{\sigma_{12}}{\mu_2} \left( -0.0008 + 0.0039 \cdot \log_{(10)} \frac{\nu_1}{\nu_2} \right) \quad (10)$$

$$V_{cr(2)} = \frac{\sigma_{12}}{\mu_2} \left( -0.0007 + 0.0034 \cdot \log_{(10)} \frac{\nu_1}{\nu_2} \right) \quad (11)$$

These relationships clearly show, that the critical flow velocity in the oil – water system is influenced by: interfacial tension, the viscosity of the fluids and, indirectly, their specific densities.



Rys. 9. Dimensionless relation between capillary number (Ca) and ratio of kinematic viscosities  $\nu_1/\nu_2$

### 5. Summary

Based on the author’s investigations, the critical conditions leading to the instability of the silicon oil-water

system interfacial boundary and the occurrence of the lighter phase drops entrainment phenomenon, explained by the KHI mechanism, were determined. The silicon oils taken for the tests were characterized by viscosities covering a wide range of liquid slags occurring in steelmaking processes. The laboratory tests and numerical simulations exhibited good agreement in the evaluation of the velocity fields of water flowing in the facility under investigation. This allowed the critical velocity at the moment of oil drop detachment to be established for all cases of silicon oils used. As the water velocities in the layers, where oil drop detachment occurred, were difficult to be set a single level, therefore the range corresponding to the maximum and minimum values was adopted. The results obtained on this basis were well approximated by the mathematical equation, describing the variation in the capillary number with variation in oil-to-water kinematic viscosity ratio (Fig. 9). Thus, two equations – (10) and (11) – were obtained, which expressed the manner in which the critical velocity changed in the silicon oil-water system, depending on viscosity, interfacial tension, – indirectly – specific density and. As the ranges of variations of specific density and interfacial tension in the examined cases did not differ significantly, therefore it is visible, that the lighter phase viscosity had the most significant influence on the variation of the critical velocity. It was found that with increasing viscosity, the critical velocity increased. Theoretical models represented with equations (1) and (2) do not consider viscosity (inviscid fluids), therefore only the results for the examined oils of the lowest viscosity are close to the results of calculations from the theoretical model. The empirical models quoted from the literature, formulae (3), (4) and (5), allow for the effect of the lighter and heavier phase viscosities and other parameters of the investigated system, e.g. the thickness of the lighter layer. Empirical formula (4) yields the correct trend in the increase of the critical velocity with increasing oil viscosity; however, the calculated values are unrealistically large. The closest to the author’s investigation results is empirical model (5). The discrepancies between the author’s investigations and other empirical models provided in the literature can be explained by the following factors: the different experimental technique employed, the differences in interfacial boundary geometry and the sensitivity of the phenomenon in question on the interfacial tension and liquids viscosity.

It is also worth noting, that the Volume of Fluid multi-phase model employed to numerical simulation of the examined phenomenon, made it possible to define the picture of the oil-water interfacial boundary, depending on the variation in water flow rate. As a result, the moment of oil drop detachment could be captured. Both in the laboratory tests and in numerical simulation, Polsil OM20 oil drops were found to detach immediately after the cylindrically curved channel outlet for the water flow rate equal to 8.0 l/min.

The derived relationships (10) and (11) can be useful for the determination of the limiting velocities of steel casting in the mould, using the theory of similarity, with the aim of avoiding the entrainment of liquid slag drops and their passing into the steel.

The next planned stage of investigation undertakes to identify the effect of lighter phase layer thickness on the formation of the interfacial boundary, and to determine the values of the critical drops entrainment velocity, at the instability of the phase.

## REFERENCES

- [1] K.C. Mills, A.B. Fox, *ISIJ Int.* **43**, 1479 (2003)
- [2] K.C. Mills, *ISIJ Int.* **56**, 1 (2016)
- [3] K.C. Mills, *ISIJ Int.* **56**, 14 (2016)
- [4] S-M. Cho, S-H. Kim, B.G. Thomas, *ISIJ Int.* **54**, 845 (2014)
- [5] R. Liu, B.G. Thomas, J. Sengupta, S.D. Chung, M. Trinh, *ISIJ Int.* **54**, 2314 (2014)
- [6] P.R. Scheller, R. Hagemann, *Archiv. of Metal. and Mater.* **57**, 283 (2012)
- [7] R. Hagemann, R. Schwarze, H.P. Heller, P.R. Scheller, *Metall. Mater. Trans. B* **44B**, 80 (2013)
- [8] P. Sulasalmi, A. Kärnä, T. Fabritius, J. Savolainen, *ISIJ Int.* **49**, 1661 (2009)
- [9] L.C. Hibbeler, R. Liu, B.G. Thomas, 7<sup>th</sup> European Continuous Casting Conf., 1, Düsseldorf (2011)
- [10] K.E. Swartz, L.C. Hibbeler, B.P. Joyce, B.G. Thomas, in: K.D. Hickey, *Proceedings of the Iron & Steel Technology Conference*, 1865, Indianapolis (2014)
- [11] M. Iguchi, J. Yoshida, T. Shimizu, Y. Mizuno, *ISIJ Int.* **40**, 685 (2000)
- [12] S.Chandrasekhar, *Hydrodynamic and Hydromagnetic Stability*, Dover Publications, New York, 1981
- [13] L.M. Milne-Thompson, *The Macmillan Press Ltd., Theoretical Hydrodynamics*, 5th ed., London 1968
- [14] A. Cwudziński, *Steel Res. Int.* **85**, 902 (2014).

